GEOPHYSICS, VOL. 66, NO. 6 (NOVEMBER-DECEMBER 2001); P. 1774–1780, 9 FIGS.

A new method for shape and depth determinations from gravity data

El-Sayed M. Abdelrahman, Tarek M. El-Araby, Hesham M. El-Araby, and Eid R. Abo-Ezz*

ABSTRACT

We have developed a simple method to determine simultaneously the shape and depth of a buried structure from residualized gravity data using filters of successive window lengths. The method is similar to Euler deconvolution, but it solves for shape and depth independently. The method involves using a relationship between the shape factor and the depth to the source and a combination of windowed observations. The relationship represents a parametric family of curves (window curves). For a fixed window length, the depth is determined for each shape factor. The computed depths are plotted against the shape factors, representing a continuous, monotonically increasing curve. The solution for the shape and depth of the buried structure is read at the common intersection of the window curves. This method can be applied to residuals as well as to the Bouguer gravity data of a short or long profile length. The method is applied to theoretical data with and without random errors and is tested on a known field example from the United States. In all cases, the shape and depth solutions obtained are in good agreement with the actual ones.

INTRODUCTION

One of the most important exploration problems is estimating the shape and depth of a buried structure. Different methods have been developed to determine the shape and depth of the buried structure from gravity data. The methods generally fall into one of two categories. The first category is continuous modeling methods (Tanner, 1967; Cordell and Henderson, 1968), which require density information as part of the input, along with some depth information obtained from geological and/or other geophysical data. Thus, the resulting model can vary widely, depending on these factors, and still give a calculated curve in close agreement with the observed data. The second category is fixed simple geometry methods, in which the sphere, horizontal-cylinder, and vertical-cylinder models determine the shape and depth of the buried structures from residuals and/or observed data. The models may not be entirely geologically realistic, but usually approximate equivalence is sufficient to determine whether the form and magnitude of the calculated gravity effects are close enough to those observed to make the geological interpretation reasonable. The advantage of fixed geometry methods over continuous modeling methods is that they require neither density nor depth information, and they can be applied if little or no factual information other than the gravity data is available. For interpreting isolated simple source bodies, fixed geometry methods can be both fast and accurate.

Several methods have been developed to interpret gravity data using a fixed simple geometry. The methods include, for example, use of the half-g_{max} rule (Nettleton, 1976), Kelvin transformation (Nedelkov and Burnev, 1962), Fourier transform (Odegard and Berg, 1965), least-squares minimization approaches (Gupta, 1983; Abdelrahman, 1990; Abdelrahman and El-Araby, 1993a; Abdelrahman and Sharafeldin, 1995a), ratio techniques (Bowin et al., 1986; Abdelrahman et al., 1989), Mellin transform (Mohan et al., 1986), and the Euler deconvolution technique (Klingele et al., 1991; Zhang et al., 2000). These methods all require prior knowledge of a simple shape that can be used to approximate the true form of the source.

Efforts have been made to identify the shape of a source for observed data. Shaw and Agarwal (1990) indicate that the Walsh transform can be used. Abdelrahman and Sharafeldin (1995b) have developed a least-squares minimization approach to determine the shape and depth of the buried structure from residual gravity data. Nandi et al. (1997) use quadratic equations to predict the shapes of sources with simple geometry from the gravity anomaly and its gradient. However, the accuracy of the results obtained by these methods depends on the accuracy with which the residual anomaly can be separated from observed gravity anomaly.

Manuscript received by the Editor February 15, 2000; revised manuscript received January 17, 2001.
*Cairo University, Geophysics Department, Giza, Egypt.

On the other hand, Abdelrahman and El-Araby (1993b) show that correlation factors between successive least-squares residual gravity anomalies from a buried vertical cylinder, horizontal cylinder, and sphere can be used to extract depth and regional field information and simultaneously to define the shape of the buried structure. The drawback with this approach is that it cannot be applied to interpret all gravity data points acquired over a large area of the buried structure, i.e., from the long segment of the gravity profile around the gravity anomaly maximum. In this case, the correlation factors are independent of the depth, shape, and size of the buried structure and are only a function of the orders of the regional polynomial used (Abdelrahman et al., 1985). Effective and simple interpretation procedures for shape and depth determination based on the analytical expression of second moving average residual gravity anomalies are yet to be developed.

We have developed a new, simple method of deriving the depth and shape of the sources of gravity anomalies of short or long profile lengths in the presence of regional variations. The method is superior to other published fixed geometry methods because it involves using simple models convolved with the same second moving average filter as applied to the observed gravity data. These techniques can be quite powerful when interpreting isolated anomalies with relative simple source geometries such as spheres and cylinders. The validity of the method is tested on theoretical examples and on a field example from the United States.

FORMULATION OF THE PROBLEM

Following Abdelrahman and El-Araby (1993a), the general gravity anomaly expression produced by most geological structures is given by

$$g(X_i, Z, q) = \frac{A}{\left(X_i^2 + Z^2\right)^q}, \tag{1}$$

where q is the shape (shape factor), Z is depth, X is the position coordinate, and A is an amplitude coefficient related to the radius and density contrast of the buried structure. Examples of the shape factor for the semiinfinite vertical cylinder (3-D), horizontal cylinder (2-D), and sphere (3-D) are 0.5, 1.0, and 1.5, respectively. Also, the shape factor for the finite vertical cylinder is approximately 1.0 (Abdelrahman and El-Araby, 1993b). The shape factor (q) approaches zero as the structure becomes a flat slab and approaches 1.5 as the structure becomes a perfect sphere (point mass).

Let us consider five observation points ($X_i - 2s$, $X_i - s$, X_i, $X_i + s$, and $X_i + 2s$) along the anomaly profile where $s = 1, 2, \ldots,$ M spacing units and is called the window length. The first moving average residual gravity anomaly $R_1(X_i, Z, q, s)$ at point X_i is defined as (Abdelrahman and El-Araby, 1993a)

$$R_1(X_i, Z, q, s) = \frac{A}{2}\left[2\left(X_i^2 + Z^2\right)^{-q} - \left(\left((X_i - s)^2 + Z^2\right)^{-q} + \left((X_i + s)^2 + Z^2\right)^{-q}\right)\right]. \tag{2}$$

The second moving average residual gravity anomaly $R_2(X_i, Z, q, s)$ at point X_i is

$$R_2(X_i, Z, q, s) = \frac{A}{4}\left[6\left(X_i^2 + Z^2\right)^{-q} - 4\left((X_i - s)^2 + Z^2\right)^{-q} - 4\left((X_i + s)^2 + Z^2\right)^{-q} + \left((X_i - 2s)^2 + Z^2\right)^{-q} + \left((X_i + 2s)^2 + Z^2\right)^{-q}\right]. \tag{3}$$

For all shape factors (q), equation (3) gives the following value at $X_i = 0$:

$$A = \frac{2R_2(0)}{\left[3Z^{-2q} - 4(s^2 + Z^2)^{-q} + (4s^2 + Z^2)^{-q}\right]}. \tag{4}$$

Using equations (3) and (4), we obtain the following normalized equation at $X_i = s$:

$$\frac{R_2(s)}{R_2(0)} = \frac{\left[7(s^2 + Z^2)^{-q} - 4Z^{-2q} - 4(4s^2 + Z^2)^{-q} + (9s^2 + Z^2)^{-q}\right]}{2\left[3Z^{-2q} - 4(s^2 + Z^2)^{-q} + (4s^2 + Z^2)^{-q}\right]}. \tag{5}$$

Equation (5) is independent of the amplitude coefficient (A). Let $F = (R_2(s)/R_2(0))$. Then from equation (5) we obtain

$$Z = \left[\frac{4}{\left[7(s^2 + Z^2)^{-q} - 4(4s^2 + Z^2)^{-q} + (9s^2 + Z^2)^{-q}\right] - 2F^*\left[3Z^{-2q} - 4(s^2 + Z^2)^{-q} + (4s^2 + Z^2)^{-q}\right]}\right]^{1/2q}. \tag{6}$$

Equation (6) can be solved for Z using a simple iterative method (Demidovich and Maron, 1973). However, the accuracy of the results obtained using this equation depends upon the accuracy to which the shape factor (q) can be assumed or determined from other geological and geophysical data.

SOLUTION USING THE WINDOW CURVES METHOD

Equation (6) can be used not only to determine the depth but also to estimate the shape of the buried structure simultaneously. The procedure is as follows.

1) Digitize the anomaly profile at several points, including the central point, $X_i = 0$.
2) Subject the digitized values to a separation technique using the second moving average method. The numerical second moving average value at point X_i is computed from observed gravity data $g(X_i)$ using the equation

$$R_2(X_i) = \frac{6g(X_i) - 4g(X_i - s) - 4g(X_i + s) + g(X_i - 2s) + g(X_i + 2s)}{4}. \tag{7}$$

3) Apply several second moving average filters of successive window lengths to the input data. Specifiy the second moving average windows by using $s = 1, 2, 3, \ldots, M$ spacing units. In this way, several numerical second moving average profiles are obtained. Then apply equation (6) to each of the second moving average residual profiles, yielding depth solutions for all q values. Plot the computed depths against the shape factor, representing a monotonically increasing window curve.

   The window curves should intersect at a point, i.e., the value of q at the point of intersection is the shape factor, and the value of Z at the point of intersection gives the depth to the buried structure. The window curves should intersect at the true solution because equation (6) has only two unknowns (q, Z). Theoretically, any two curves associated with two different values of s are enough to simultaneously determine Z and q. In practice, more than two values of s are desirable because of the presence of noise in data.

Our method is similar to the Euler deconvolution method (Klingele et al., 1991; Marson and Klingele, 1993). Both techniques lead to a relationship involving the source depth and a factor related to the source nature. However, in our method the shape factor and the depth are determined simultaneously, whereas in Euler deconvolution there is ambiguity in selecting the correct structural index to then compute an accurate source depth.

THEORETICAL EXAMPLES

We computed three different composite gravity fields, each consisting of the combined effect of a local structure (semi-infinite vertical cylinder, horizontal cylinder, and sphere), and added a regional polynomial component. The model equations representing the model and the regional anomalies are vertical cylinder + first-order regional, or

$$\Delta g_1 = \frac{200}{\left(X_i^2 + 2^2\right)^{0.5}} + 2X_i + 80, \qquad (8)$$

horizontal cylinder + second-order regional, or

$$\Delta g_2(X_i) = \frac{600}{\left(X_i^2 + 4^2\right)} + 0.1X_i^2 + 2X_i + 5, \qquad (9)$$

and sphere + third-order regional, or

$$\Delta g_3(X_i) = \frac{10\,000}{\left(X_i^2 + 6^2\right)^{1.5}} + 0.01X_i^3 + 0.1X_i^2 + X_i + 5. \qquad (10)$$

The three composite gravity fields are shown in Figure 1.

Each composite field (Δg) was subjected to our new second moving average technique. Three successive second moving average windows ($s = 2$, 3, and 4 km) were applied to each set of input data. The second moving average residual gravity anomalies thus obtained are shown in Figure 2. Each of the resulting moving average profiles was analyzed based on equation (6). For each window length, a depth value was determined for all shape values, and a window curve was plotted, illustrating the relation between the depth and shape. The results are summarized in Figure 3.

The correct solution for the q theoretical models occurs at the common intersection of the window curves. Figure 3a shows

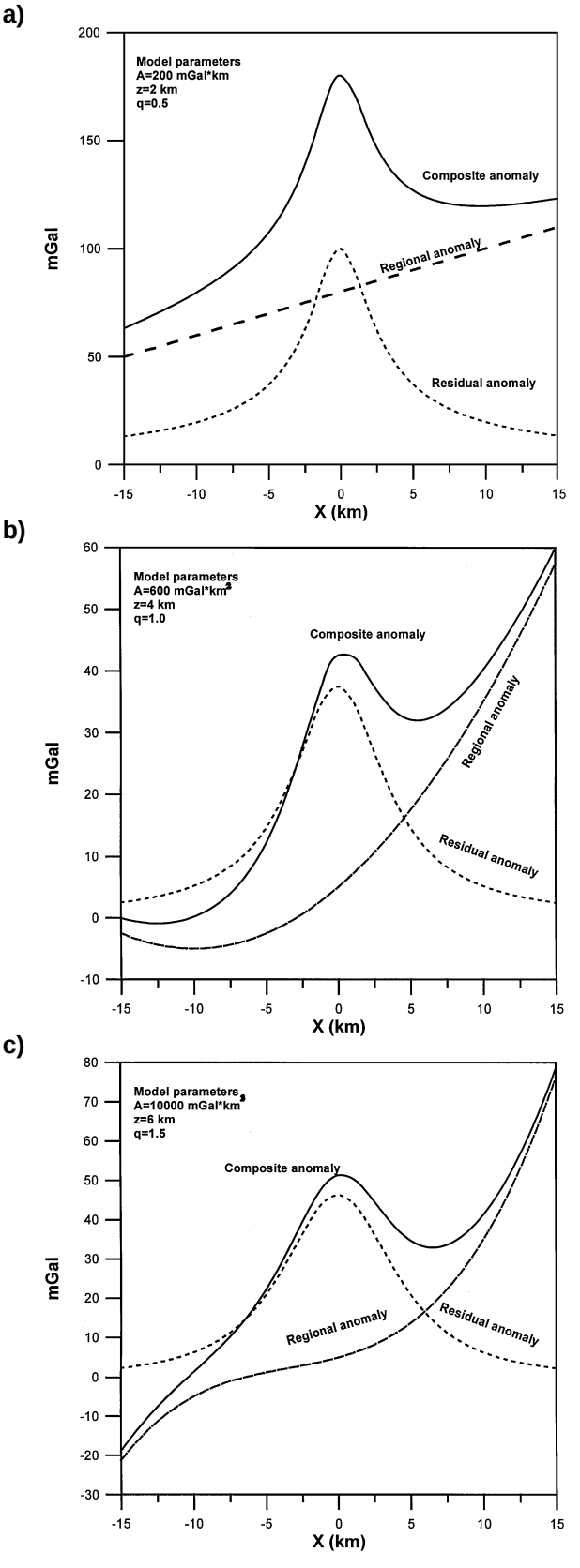

FIG. 1. Composite gravity anomaly (a) Δg_1 of a buried vertical cylinder and first-order regional anomaly as obtained from equation (8), (b) Δg_2 from equation (9), and (c) Δg_3 from equation (10).

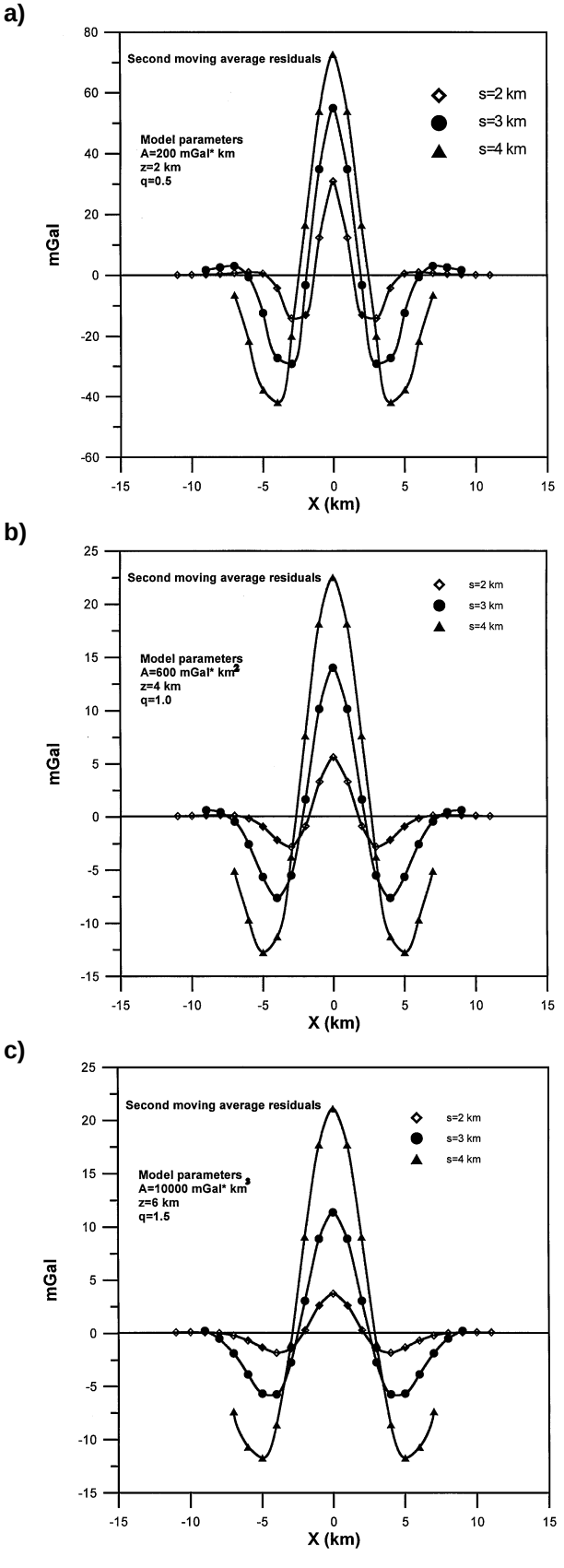

FIG. 2. Second moving average residual gravity anomalies for $s = 2, 3$, and 4 km as obtained from gravity anomalies (a) Δg_1, (b) Δg_2, and (c) Δg_3.

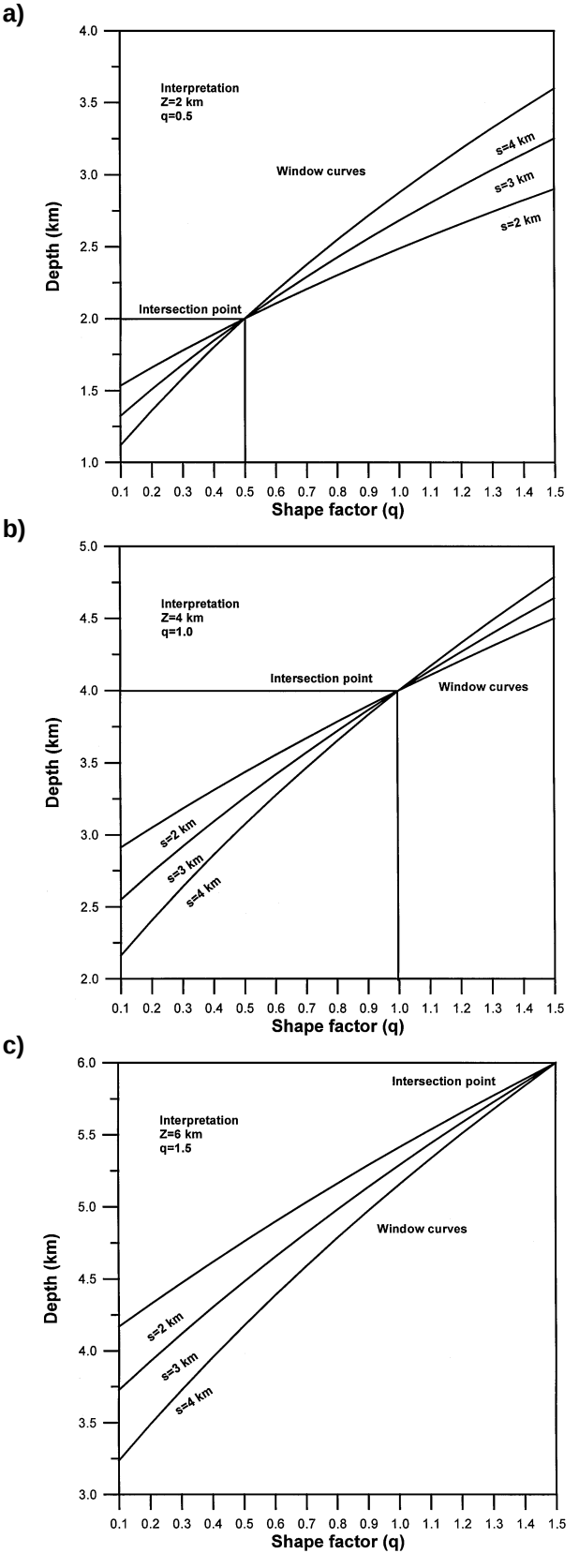

FIG. 3. Family of window curves of Z as a function of q for $s = 2, 3$, and 4 km using the present approach as obtained from gravity anomalies (a) Δg_1 for $q = 0.5$ and $Z = 2$ km; (b) Δg_2 for $q = 1.0$ and $Z = 4$ km; and (c) Δg_3 for $q = 1.5$ and $z = 6$ km.

the intersection at the correct location $q = 0.5$ and $Z = 2$ km. Figure 3b shows the window curves intersect at the correct point $q = 1$ and $Z = 4$ km. Figure 3c shows the intersection at the correct location $q = 1.5$ and $Z = 6$ km. In all cases, the solution for the shape and depth are in excellent agreement with the parameters given in model equations (8), (9), and (10). The method is also independent of the regional component present in the data because the second moving average filter removes its effect.

Moreover, random errors of 10% were added to each composite gravity anomaly Δg to produce three different noisy anomalies. Each noisy anomaly is subjected to a separation technique using the second moving average method. Successive second moving average windows were applied to the noisy input data to obtain successive second moving average residual profiles (Figure 4). Adapting the same interpretation procedure used in the above examples, the results are shown in Figure 5.

When the data are noisy, the window curve intersections are subject to interpretation. In the case of the vertical cylinder model, the window curves intersect each other in a narrow region where $0.62 > q > 0.42$ and 2.2 km $> Z >$ 1.6 km (Figure 5a). The central point of this intersection (intersection point) occurs at approximate location $q = 0.51$ and $Z = 1.98$ km. In the case of the horizontal cylinder model, the window curves also intersect at a narrow region where $1.2 > q > 0.95$ and 4.7 km $> Z >$ 4.0 km (Figure 5b). The central point of the region occurs at the approximate location $q = 1.1$ and $Z = 4.4$ km. On the other hand, in the case of the sphere model, the curves intersect each other in a region where $1.5 > q > 1.35$ and 5.7 km $> Z >$ 5.4 km (Figure 5c). The central point of this region is located at $q = 1.45$ and $Z = 5.6$ km. In all cases, the solutions for the shape and depth are still in very good agreement with the parameters given in the model equations (8), (9), and (10), respectively. This demonstrates that our method will give reliable results even when the gravity data contain measurement errors.

FIELD EXAMPLE

The Bouguer gravity map of the Humble Dome near Houston (Nettleton, 1962, his Figure 22) is shown in Figure 6. A gravity profile of 20 km along line AA', displayed in Figure 7, has been digitized at an interval of 0.25 km. The Bouguer anomalies thus obtained have been subjected to a separation technique using the second moving average method. Filters were applied in four successive windows ($s = 1.5, 1.75, 2$, and 2.25 km). In this way, four second moving average residual anomaly profiles were obtained (Figure 8). The same procedure described for the synthetic examples was used to estimate the shape and depth of the salt dome. The results are plotted in Figure 9.

Figure 9 shows the window curves can be interpreted to intersect at a point where the depth is about 4.95 km and at $q = 1.5$. This suggests that the shape of the salt dome resembles a sphere or, practically, a 3-D source with a hemispherical roof and root. This may indicate that the salt flow toward the dome continued until the salt formation in its synclinal rim was exhausted. This result is generally in good agreement with the dome form estimated from drilling top and contact (Nettleton, 1976, his Figure 8–16). This anomaly has been interpreted by

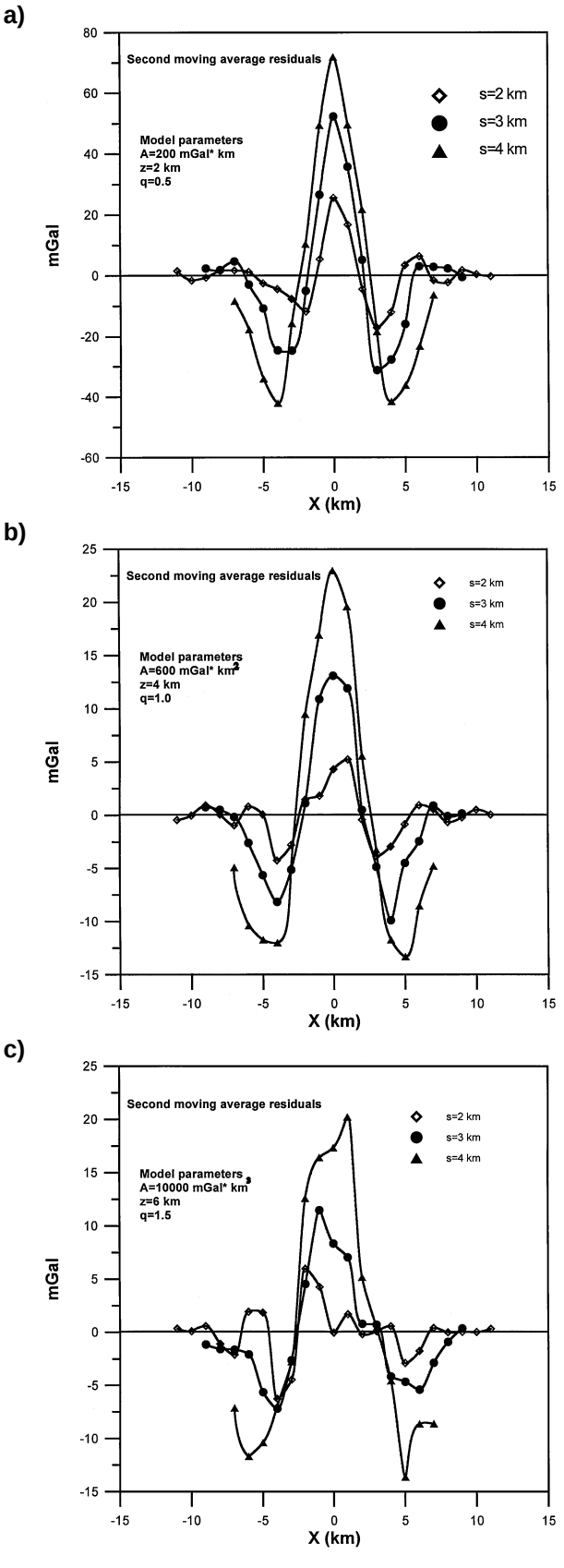

FIG. 4. Second moving average residual gravity anomalies for $s = 2, 3$, and 4 km after adding 10% random errors to the data as obtained from (a) Δg_1, (b) Δg_2, and (c) Δg_3.

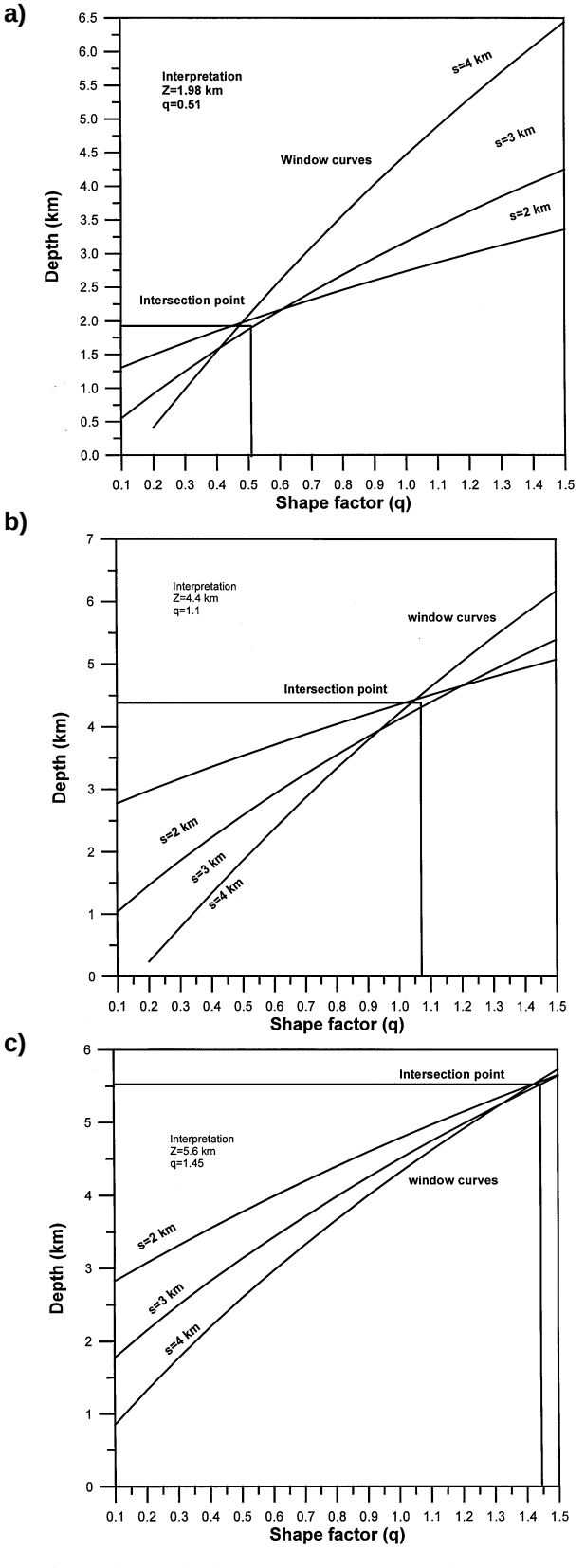

FIG. 5. Family of window curves of Z as a function of q for $s = 2$, 3, and 4 km after adding 10% random errors to the data using the present approach as obtained from (a) Δg_1 for $q = 0.51$ and $z = 1.98$ km, (b) Δg_2 for $q = 1.1$ and $z = 4.4$ km, and (c) Δg_3 for $q = 1.45$ and $z = 5.6$ km.

assuming a spherical source to determine the depth to the center of the salt body. The result of the present study, based on a spherical target, and those obtained from applying the half-g_{max} rule method (Nettleton, 1976), the Mellin transform technique (Mohan et al., 1986), and the least-squares method (Abdelrahman and El-Araby, 1993a) are in excellent agreement.

CONCLUSIONS

The problem of determining shape and depth from gravity data of long or short profile length can be solved using the present method for simple anomalies. The window curves method is very simple to execute and works well even when the data contain noise. The method involves using simple models convolved with the same second moving average filter as applied to the observed gravity data. As a result,

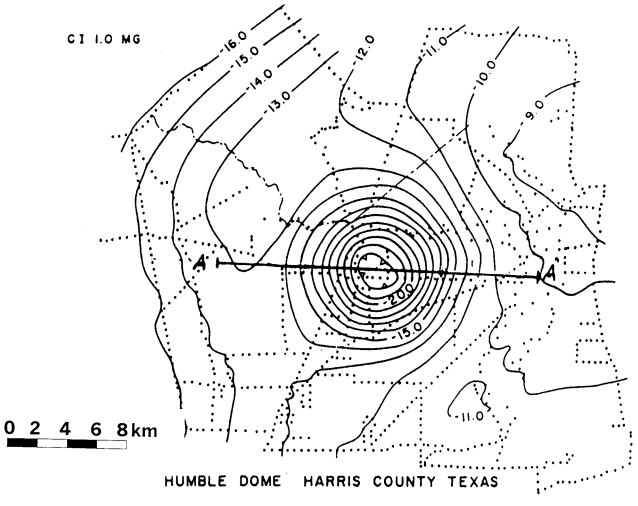

FIG. 6. Bouguer gravity map, Humble salt dome, Harris County, Texas (Nettleton, 1962). Computations are made along profile AA'.

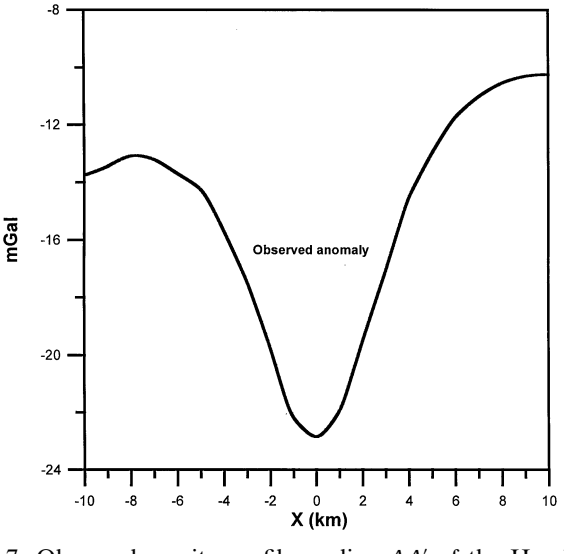

FIG. 7. Observed gravity profile on line AA' of the Humble dome near Houston.

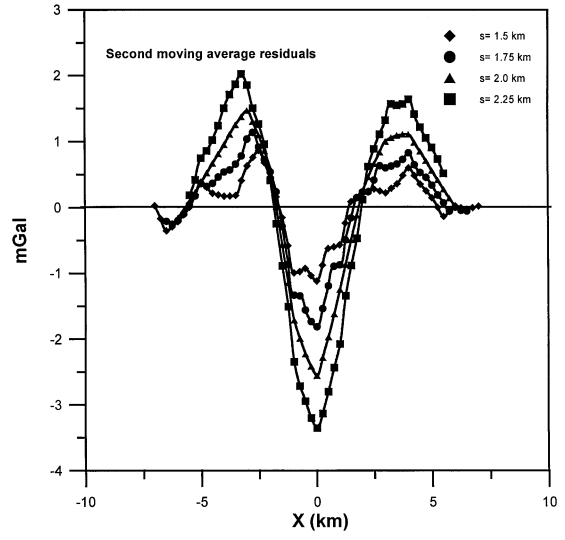

FIG. 8. Second moving average residual gravity anomalies on line AA' of the Humble dome for $s = 1.5, 1.75, 2$, and 2.25 km.

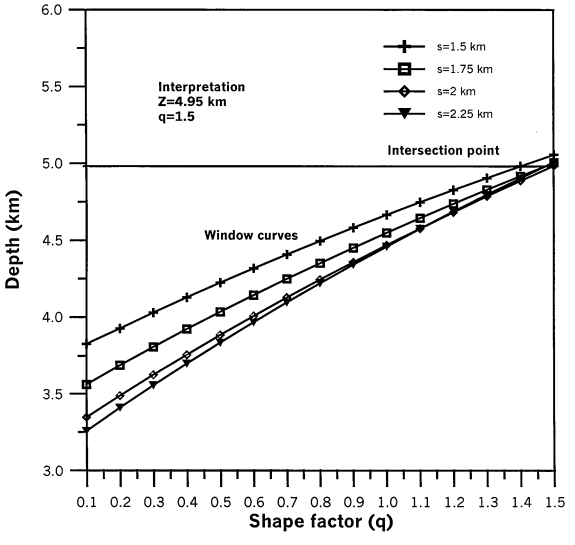

FIG. 9. Family of window curves of Z as a function of q for $s = 1.5, 1.75, 2$, and 2.25 km as obtained from the Humble gravity anomaly profile using our approach. Estimates of q and Z are, respectively, 1.5 and 4.95 km.

our method can be applied not only to residuals but also to measured gravity data.

Given its relative strength, our work complements the existing methods of shape and depth determination and overcomes some of their shortcomings. It is especially good when interpreting isolated anomalies such as salt domes that potentially have simple geometries. The method is developed to derive shape and depth simultaneously while removing the regional trend from gravity data. Obtaining these two parameters together is a powerful means to gain new geological insight about the subsurface.

ACKNOWLEDGMENTS

The authors thank the editors and the two capable reviewers for their excellent suggestions. Many thanks to David A. Chapin, the associate editor, for his keen interest, valuable comments on the manuscript, and improvements to this work.

REFERENCES

Abdelrahman, E. M., 1990, Discussion on "A least-squares approach to depth determination from gravity data" (O. P. Gupta, 1983, Geophysics, **48**, 357–360): Geophysics, **55**, 376–378.

Abdelrahman, E. M., and El-Araby, T. M., 1993a, A least-squares minimization approach to depth determination from moving average residual gravity anomalies: Geophysics, **59**, 1779–1784.

———1993b, Shape and depth solutions from gravity data using correlation factors between successive least-squares residuals: Geophysics, **59**, 1785–1791.

Abdelrahman, E. M., and Sharafeldin, S. M., 1995a, A least-squares minimization approach to shape determination from gravity data: Geophysics, **60**, 589–590.

———1995b, A least-squares minimization approach to depth determination from numerical horizontal gravity gradients: Geophysics, **60**, 1259–1260.

Abdelrahman, E. M., Bayoumi, A. I., Abdelhady, Y. E., Gobashy, M. M., and El-Araby, H. M., 1989, Gravity interpretation using correlation factors between successive least-squares residual anomalies: Geophysics, **54**, 1614–1621.

Abdelrahman, E. M., Riad, S., Refai, E., and Amin, Y., 1985, On the least-squares residual anomaly determination: Geophysics, **50**, 473–480.

Bowin, C., Scheer, E., and Smith, W., 1986, Depth estimates from ratios of gravity, geoid, and gravity gradient anomalies: Geophysics, **51**, 123–136.

Cordell, L., and Henderson, R. G., 1968, Iterative three-dimensional solution of gravity anomaly data using a digital computer: Geophysics, **33**, 596–601.

Demidovich, B., and Maron, I. A., 1973, Computational mathematics: Mir Publ.

Gupta, O. P., 1983, A least-squares approach to depth determination from gravity data: Geophysics, **48**, 375–360.

Klingele, E. E., Marson, I., and Kahle, H. G., 1991, Automatic interpretation of gravity gradiometric data in two dimensions: Vertical gradients: Geophys. Prosp., **39**, 407–434.

Marson, I., and Klingele, E. E., 1993, Advantages of using the vertical gradient of gravity for 3-D interpretation: Geophysics, **58**, 1588–1595.

Mohan, N. L., Anandababu, L., and Roa, S., 1986, Gravity interpretation using the Melin transform: Geophysics, **51**, 114–122.

Nandi, B. K., Shaw, R. K., and Agarwal, B. N. P., 1997, A short note on identification of the shape of simple causative sources from gravity data: Geophys. Prosp., **45**, 513–520.

Nedelkov, I. P., and Burnev, P. H., 1962, Determination of gravitational field in depth: Geophys. Prosp., **10**, 1–18.

Nettleton, L. L., 1962, Gravity and magnetic for geologists and seismologists: AAPG Bulletin, **46**, 1815–1838.

———1976, Gravity and magnetics in oil prospecting: McGraw-Hill Book Co. (Div. of McGraw-Hill, Inc.).

Odegard, M. E., and Berg, J. W., 1965, Gravity interpretation using the Fourier integral: Geophysics, **30**, 424–438.

Shaw, R. K., and Agarwal, S. N. P., 1990, The application of Walsh transform to interpret gravity anomalies due to some simple geometrically shaped causative sources: A feasibility study: Geophysics, **55**, 843–850.

Tanner, J. G., 1967, An automated method of gravity interpretation: Geophys. J. Roy. Astr. Soc., **13**, 339–347.

Zhang, C., Mushayandebvu, M. F., Reid, A. B., Fairhead, J. D., and Odegard, M. E., 2000, Euler deconvolution of gravity tensor gradient data: Geophysics, **65**, 512–520.